

EXPERIMENTAL ANALYSIS OF PERFORMANCE AND PREDICTION OF OPTIMAL COMPRESSION RATIO, IGNITION TIMING, AND EGR RATIO FOR 80% HYDROGEN DIRECT INJECTION WITH 20% ETHANOL ON SPARK IGNITION ENGINE

M. Velliangiri, M. Karthikeyan, A. Karthikeyan, G. Sureshkannan

Assistant Professor, Associate Professor Department of Mechanical Engineering- Coimbatore Institute of Technology, Coimbatore-14.

velliangiri69@gmail.com, karthikeyan.m@cit.edu.in, karthikeyanmech@cit.edu.in, sureshkannan.mech.cit@gmail.com

Abstract

This study investigates the performance of a Spark Ignition (SI) engine fueled with an 80% hydrogen direct injection with 20% ethanol manifold injection and focusing on optimizing the compression ratio (CR), ignition timing (IT), and Exhaust Gas Recirculation (EGR) ratio for improved engine efficiency and reduced emissions. The results indicate that increasing the CR from 8.0 to 11.5 boosts engine power from 28.5 kW to 31.31 kW and reduces specific fuel consumption (SFC) to a minimum of 0.35 kg/kWh at CR 11.5. However, NO_x emissions rise from 0.651 ppm to 233.18 ppm with higher CRs. Optimal ignition timing of 10° before Top Dead Center (TDC) enhances performance while balancing NO_x emissions and peak pressure. EGR also impacts engine performance, with higher EGR reducing power and increasing SFC. The optimal configuration for the 80% hydrogen and 20% ethanol blend is found to be CR 10.5, IT at 10° before TDC, and EGR at 10%, offering a balanced performance with good power output, reduced fuel consumption, and manageable emissions.

Keywords: *Hydrogen-Ethanol Blend, Compression Ratio, Ignition Timing, Exhaust Gas Recirculation (EGR), Spark Ignition Engine Performance.*

1. INTRODUCTION

The significance of this research lies in its contribution to advancing clean and sustainable transportation technologies through the optimization of spark ignition (SI) engines powered by an 80% hydrogen and 20% ethanol blend. By addressing key engine parameters such as compression ratio, ignition timing, and EGR ratio, the study provides critical insights into achieving higher thermal efficiency, reduced fuel consumption, and improved combustion stability. The use of hydrogen and ethanol-renewable and low-emission fuels, presents a viable alternative to conventional fossil fuels, significantly reducing harmful emissions such as CO₂, NO_x, CO, and HC [1,2,3,4,5,6]. Furthermore, the research offers practical solutions for integrating these alternative fuels into existing engine systems, facilitating their adoption in real-world applications. This study also highlights the role of hydrogen-ethanol blends in mitigating the challenges of pre-ignition, knocking, and thermal management, paving the way for their use in high-efficiency, low-emission engines [6,7,8,9,10]. Overall, this research supports global efforts to reduce greenhouse gas emissions and transition to sustainable energy systems, aligning with environmental regulations and energy security goals.

1.1 Literature Review

Hydrogen and ethanol have emerged as promising alternative fuels for internal combustion engines due to their environmental and performance benefits. Their high-octane numbers, lean burn capabilities, and potential to reduce greenhouse gas emissions make them viable candidates for blending with traditional fuels [11,12,13,14].

1.2 Hydrogen as a Fuel

Hydrogen is recognized for its high energy content and zero carbon emissions during combustion. Verhelst and Wallner (2009) provided a comprehensive review of hydrogen-fueled internal combustion

engines (ICEs), highlighting challenges such as pre-ignition and knocking, especially under high compression ratios. The use of hydrogen in SI engines requires careful optimization of ignition timing and compression ratio to achieve efficient combustion (Bari & Esmaeil, 2010). Studies also indicate that hydrogen addition enhances flame speed and extends lean operating limits, improving thermal efficiency (Milton & Keck, 1984) [15,16,17,18,19].

1.3 Ethanol as a Fuel

Ethanol has gained attention for its renewable origin and ability to reduce emissions. Abdel-Rahman and Osman (1997) explored ethanol-gasoline blends and found significant improvements in engine performance and emissions at optimal compression ratios. Ethanol's high latent heat of vaporization also contributes to better combustion chamber cooling, which can offset the high in-cylinder temperatures associated with hydrogen blends (Hsieh et al., 2002) [20,21,22,23,24].

1.4 Hydrogen-Ethanol Blends

Blending hydrogen and ethanol offers synergistic advantages, combining the high energy density of hydrogen with ethanol's cooling properties. Pal and Sen (2018) demonstrated the benefits of hydrogen-ethanol blends in spark ignition engines, noting improved brake thermal efficiency (BTE) and reduced NO_x emissions under optimized conditions. The blend ratio significantly influences combustion characteristics, necessitating precise control of parameters like compression ratio, ignition timing, and exhaust gas recirculation (EGR) [25,26,27,28,29].

1.5 Compression Ratio Optimization

The optimal compression ratio is critical for maximizing the thermal efficiency of hydrogen-ethanol blends. Studies by Çelik (2008) showed that higher compression ratios improve fuel efficiency but may increase the risk of knocking, especially in hydrogen-rich blends. This necessitates balancing the compression ratio to leverage the high knock resistance of ethanol while mitigating pre-ignition risks from hydrogen [30].

1.6 Ignition Timing and Combustion Control

Ignition timing plays a pivotal role in optimizing the performance of SI engines. Kim and Lee (2013) explored the effect of advanced ignition timing on hydrogen-ethanol blends, demonstrating enhanced power output and reduced cyclic variation. Advanced ignition timing maximizes the combustion pressure while maintaining stable operation, particularly under lean burn conditions [22,23,24,25,26].

1.7 Exhaust Gas Recirculation (EGR)

EGR is widely employed to control NO_x emissions in SI engines. Mahla and Chauhan (2018) analyzed the impact of EGR on hydrogen-ethanol blends, noting significant NO_x reductions with minimal trade-offs in efficiency. However, excessive EGR ratios may lead to incomplete combustion and increased hydrocarbon (HC) emissions, necessitating an optimal EGR rate [30].

1.8 Performance and Emissions Analysis

The integration of hydrogen and ethanol in SI engines has shown promising results in terms of performance and emissions. Li et al. (2017) reported that an 80% hydrogen and 20% ethanol blend achieved higher BTE and lower carbon monoxide (CO) emissions compared to pure gasoline operation. EGR and precise ignition timing further enhanced combustion stability and reduced nitrogen oxides (NO_x).

1.9 Challenges and Future Directions

Despite the advantages, challenges remain in optimizing engine parameters for hydrogen-ethanol blends. The high reactivity of hydrogen necessitates advanced engine management systems to prevent knocking and pre-ignition. Additionally, the compatibility of existing engine components with

hydrogen-ethanol blends must be addressed. Future research should focus on real-time optimization techniques, such as AI-based models, to predict and adjust engine parameters dynamically. This literature review provides a foundation for understanding the importance of optimizing compression ratio, ignition timing, and EGR ratio for hydrogen-ethanol blends in spark ignition engines.

1.10 Scope of This Research

This research focuses on the experimental analysis of a spark ignition (SI) engine operating with a blend of 80% hydrogen and 20% ethanol, aiming to optimize key engine parameters such as compression ratio, ignition timing, and EGR ratio to enhance performance, combustion characteristics, and emission behavior. The study investigates the impact of compression ratios on brake thermal efficiency (BTE), specific fuel consumption (SFC), and power output while analyzing ignition timing adjustments to improve combustion stability and mitigate knock resistance. Additionally, the role of EGR in reducing NOx emissions is explored to strike a balance between emission control and performance. The research examines the flame propagation, ignition delay, and combustion duration for hydrogen-ethanol blends, comparing their emission profile, including CO₂, HC, and CO, with traditional gasoline engines. It assesses the feasibility of implementing such blends in existing engine designs and explores their potential for clean and sustainable transportation. By providing practical solutions for improving engine efficiency and reducing emissions, this study contributes to the global transition to low-carbon energy systems and sustainable alternative fuels.

2.0 FUEL PROPERTIES

Table 1: Fuel properties

Property	Hydrogen (H ₂)	Ethanol (C ₂ H ₅ OH)	80% Hydrogen + 20% Ethanol Blend
Molecular Mass (g/mol)	2.016	46.07	~45.59 (dominated by ethanol)
Density (kg/m ³)	0.0899	789	~157.87
Lower Heating Value (MJ/kg)	120	26.8	31.02
Stoichiometric AFR	34.3:1	09:01	Between 9:1 and 34.3:1
Octane Number	>130	~108-111	>120
Flame Speed (m/s)	~2.65	~0.4	Closer to hydrogen's (~2.65)
Mass Fraction - Hydrogen (H)	100%	13.04%	13.08%
Mass Fraction - Carbon (C)	0%	52.17%	52.14%
Mass Fraction - Oxygen (O)	0%	34.78%	34.76%
Flammability Limits (%)	4–75	3.3–19	Wider than ethanol's
Adiabatic Flame Temp (K)	2045	1920	Intermediate
Ignition Energy (mJ)	0.02	0.6	Closer to hydrogen's (~0.02)

The 80% hydrogen and 20% ethanol blend exhibit a unique combination of properties that leverage the high reactivity of hydrogen and the energy density of ethanol shown in Table 1. The blend's molecular mass and density are dominated by ethanol, but its combustion characteristics are largely influenced by hydrogen. With a lower heating value of 31.02 MJ/kg, the blend offers higher energy content than pure ethanol. Its stoichiometric air-fuel ratio lies between the wide range of hydrogen (34.3:1) and ethanol

(9:1), indicating flexible combustion conditions. The blend maintains a high-octane number (>120), ensuring excellent knock resistance, and features a flame speed and ignition energy closer to that of hydrogen, leading to faster and more efficient combustion. The flammability range is wider than that of ethanol, improving ignition reliability across varied conditions. Additionally, the blend has an intermediate adiabatic flame temperature and closely mirrors the elemental composition of ethanol, making it a promising fuel for high-efficiency, clean combustion applications.

The significance of this research lies in its contribution to advancing clean and sustainable transportation technologies through the optimization of spark ignition (SI) engines powered by an 80% hydrogen and 20% ethanol blend. By addressing key engine parameters such as compression ratio, ignition timing, and EGR ratio, the study provides critical insights into achieving higher thermal efficiency, reduced fuel consumption, and improved combustion stability. The use of hydrogen and ethanol-renewable and low-emission fuels, presents a viable alternative to conventional fossil fuels, significantly reducing harmful emissions such as CO_2 , NO_x , CO , and HC . Furthermore, the research offers practical solutions for integrating these alternative fuels into existing engine systems, facilitating their adoption in real-world applications. This study also highlights the role of hydrogen-ethanol blends in mitigating the challenges of pre-ignition, knocking, and thermal management, paving the way for their use in high-efficiency, low-emission engines. Overall, this research supports global efforts to reduce greenhouse gas emissions and transition to sustainable energy systems, aligning with environmental regulations and energy security goals.

3.0 EXPERIMENTAL SETUP AND METHODOLOGY

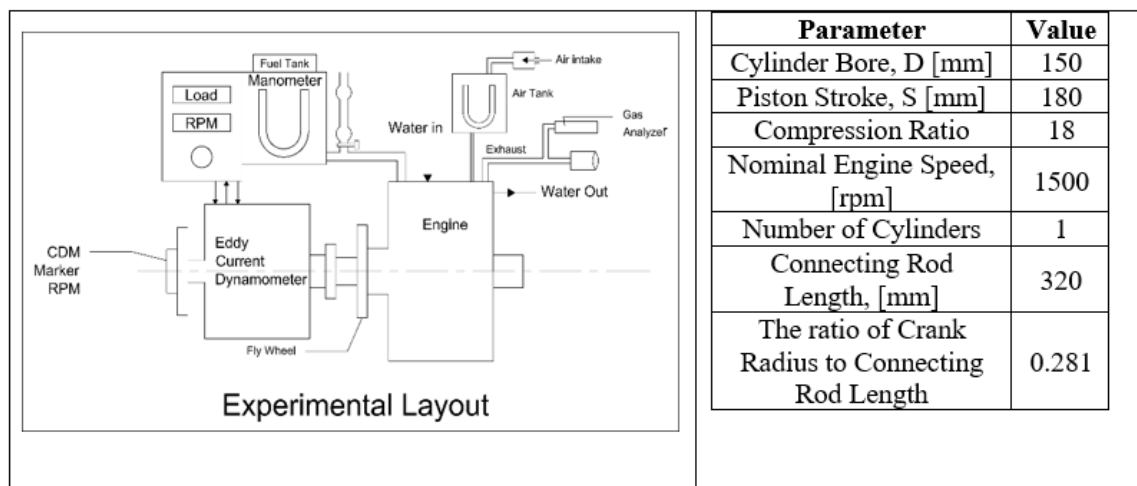


Figure 1 Experimental Layout

Experimental Setup and Methodology

The experimental setup is shown in Fig. 1. This experimental setup is used to analyze the performance, combustion characteristics, and emissions of a spark ignition (SI) engine running on a blend of 80% hydrogen and 20% ethanol. The key components of the experimental system include a single-cylinder, four-stroke engine with the following specifications: Cylinder Bore (D): 150 mm, Piston Stroke (S): 180 mm, Compression Ratio: 11.5:1, Nominal Engine Speed: 1500 rpm, Number of Cylinders: 1, Connecting Rod Length: 320 mm and Crank Radius to Connecting Rod Length Ratio: 0.281. The engine is coupled with an Eddy Current Dynamometer to measure the brake power, torque, and engine speed, as well as to apply load conditions. This dynamometer also allows the monitoring of engine performance under varying conditions. A fuel supply system is used to provide the hydrogen-ethanol blend, and a manometer measures the fuel flow. Air is introduced through the air intake system, and

exhaust gases are analyzed for emission levels, including CO₂, CO, HC, and NO_x. Additionally, a water-cooling system is employed to maintain the engine's temperature. The methodology involves preparing the hydrogen-ethanol blend and feeding it into the engine through the fuel system. The engine operates at a constant speed of 1500 rpm, and adjustments are made to key parameters like compression ratio, ignition timing, and EGR ratio to optimize performance. Emissions are measured continuously using a gas analyzer, and the effect of different ignition timings and EGR ratios on NO_x emissions is examined. Performance data such as brake thermal efficiency (BTE) and specific fuel consumption (SFC) are recorded under various load conditions using the dynamometer. The results from these experiments will allow for the determination of the optimal parameters for maximizing engine efficiency while minimizing emissions. This experimental setup provides a comprehensive framework to study the behavior of hydrogen-ethanol fuel blends in spark ignition engines, contributing to the development of cleaner, more efficient powertrains for future transportation systems.

4.0 RESULTS AND DISCUSSION

Table 2: Experimental Results

SOI	12	14	16	18	20
A/F_eq	0.62802	0.62941	0.62885	0.6283	0.62764
P_eng	30.468	30.876	31.007	31.033	30.963
SFC	0.35742	0.3527	0.35121	0.35092	0.35171
Torque	193.98	196.58	197.41	197.58	197.13
IMEP	9.2695	9.3896	9.4337	9.4566	9.4563
ON	85.378	88.227	91.14	94.451	97.497
p_max	41.543	44.414	47.174	49.991	52.883
Phi_z	59	58	58	59	59
dp/dTheta	0.74563	0.92664	1.1222	1.3334	1.5532
m_air	3.64E-02	3.64E-02	3.63E-02	3.63E-02	3.63E-02
Eta_v	0.72102	0.7205	0.71948	0.71839	0.71723
x_r	0.24212	0.24252	0.24302	0.24339	0.24388
PMEP	-	-	-	-	-
Eta_TC	0.24272	0.24764	0.24756	0.25196	0.25659
Eta_TC	0	0	0	0	0
NOx , ppm	6.15E-03	248.85	244.4	241.55	240.21
To_T	679.33	674.15	668.76	664.06	659.5
Tw_pist	443.35	445.37	447.71	450.06	452.7
A_egr	89.433	88.617	89.232	88.507	88.624
dp_ev	6.44E-02	6.51E-02	6.43E-02	6.48E-02	6.46E-02

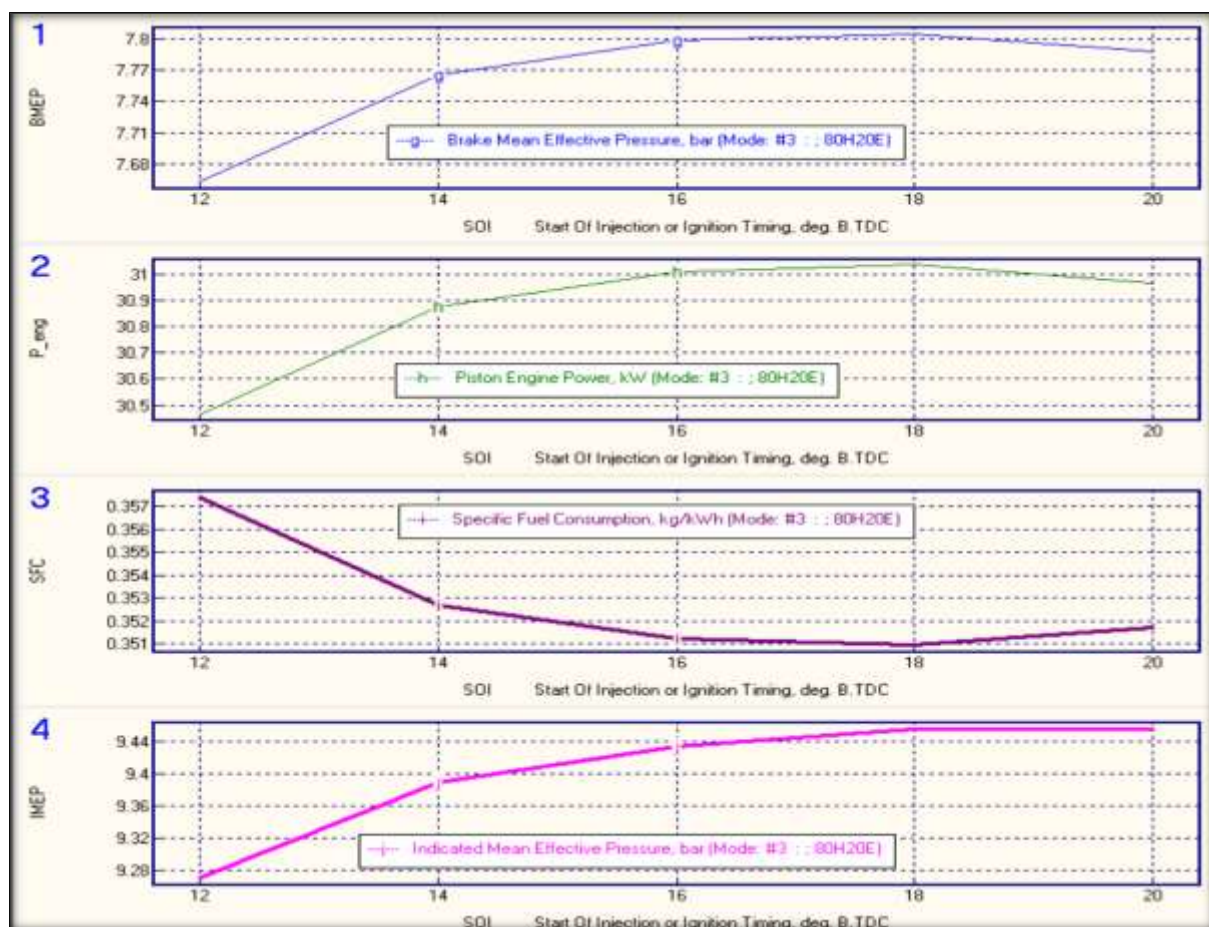


Figure 2 Performance Parameters like BMEP, IMEP, SFC, and P_{eng} comparison with variable SOI

Table 2 shows the experimental data and comparison of various SOI. Figure 2 shows the experimental analysis of an 80% hydrogen and 20% ethanol spark ignition engine reveals that varying the Start of Ignition (SOI) timing significantly influences engine performance, combustion characteristics, and emissions shown in Table.2. As the SOI advances from 12° to 20°, engine power, torque, and indicated mean effective pressure (IMEP) show a consistent increase, with optimal values achieved at SOI = 18°. At this point, torque peaks at 197.58 Nm, and SFC reaches its minimum at 0.35092 kg/kWh, indicating the most efficient combustion phase. Combustion parameters such as peak cylinder pressure (p_{max}) and pressure rise rate ($dp/d\theta$) also rise with advanced SOI, signifying more intense and complete combustion. However, this is accompanied by an increase in octane number and piston temperature, highlighting the growing thermal load on engine components. Despite improvements in power and efficiency, a significant drawback of advancing SOI is the substantial increase in NO_x emissions, from nearly zero at SOI = 12° to over 240 ppm at SOI = 18° to 20°. Volumetric efficiency slightly decreases, while the residual gas fraction and piston wall temperature increase, indicating higher thermal stress and reduced fresh charge intake. Therefore, while SOI = 18° offers the best trade-off between performance and efficiency, it comes at the cost of higher NO_x emissions. For emission-sensitive operations, a moderate ignition timing of SOI = 14°–16° may be preferable to balance power output and environmental impact. Key observations reveal that the engine's performance, combustion characteristics, emissions, and thermal effects are significantly influenced by the Start of Ignition (SOI) timing. Torque and Indicated Mean Effective Pressure (IMEP) reach their peak values at SOI = 18°

(198 Nm, 9.46 bar), highlighting this timing as optimal for performance. Specific Fuel Consumption (SFC) improves steadily up to SOI = 18° (0.351 kg/kWh) but worsens slightly at SOI = 20°. In terms of combustion, the peak pressure (p_{max}) and the pressure rise rate ($dp/d\theta$) increase with advanced SOI, reaching their maximum values at SOI = 20° (52.88 bar, 1.553 bar/°), which raises concerns about potential knocking. Emission analysis shows that nitrogen oxide (NOx) levels rise significantly with SOI advancement, peaking at 240 ppm at SOI = 20°. Thermal effects demonstrate a decrease in combustion temperature (T_o) as SOI advances, while piston temperature (T_{w_pist}) steadily increases, reaching 452.7 K at SOI = 20°. Among these findings, SOI = 18° emerges as the optimal timing, offering the best compromise between high performance, improved efficiency, and controlled emissions.

Table 3: Experimental Data with Variable Comparison Ratios

CR	8	8.5	9	9.5	10	10.5	11	11.5
A/F _{eq}	0.62751	0.62792	0.62939	0.62909	0.62893	0.62863	0.62829	0.62779
P _{eng} (kW)	28.343	29.003	29.68	30.111	30.482	30.773	31.024	31.31
SFC (kg/kWh)	0.38422	0.37547	0.36691	0.36167	0.35726	0.35388	0.35102	0.34794
Torque (Nm)	180.45	184.65	188.96	191.7	194.07	195.92	197.52	199.17
IMEP (bar)	8.6463	8.8329	9.0276	9.1578	9.2744	9.3702	9.4564	9.5324
ON	76.416	79.681	82.571	85.566	88.51	91.338	94.45	97.644
p _{max} (bar)	34.099	36.561	39.245	41.814	44.48	47.197	49.991	52.845
Phi _z (°)	59	59	58	58	58	58	59	59
dp/dTheta _a	0.71318	0.80494	0.82451	0.93707	1.0602	1.1921	1.3334	1.47532
m _{air} (kg/s)	0.03632 7	0.03634 6	0.03634 6	0.03634	0.03632 7	0.03631 6	0.03629 7	0.03627 6
Eta _v	0.72292	0.72251	0.72192	0.72112	0.7202	0.71937	0.71839	0.71743
x _r	0.25455	0.25211	0.24997	0.2481	0.24641	0.2449	0.24341	0.24195
PMEP (bar)	- 0.23058	- 0.23153	- 0.23576	- 0.23917	- 0.24401	- 0.24855	- 0.25404	- 0.25959
NOx.w, ppm	6.51E-03	277.19	271.08	267.1	258.07	250.86	241.86	233.18
To _T (K)	703.9	696.07	689.45	682.63	676.09	669.92	663.91	658.12
Tw _{pist} (K)	438.62	440.51	442.22	444.16	446.05	448.06	450.06	452.15
A _{egr} (%)	89.496	89.722	89.218	89.582	89.139	88.5	88.705	88.11
dp _{ev} (bar)	0.06475 1	0.06442 3	0.06477	0.06427 4	0.06453 9	0.06500 6	0.06464 7	0.06458 7

Table 3 shows that the Engine Power Output (P_{eng}): As the compression ratio (CR) increases, the engine power output also increases, indicating improved energy extraction from the air-fuel mixture. The highest power output of 31.31 kW is achieved at a CR of 11.5. Specific Fuel Consumption (SFC): SFC decreases with increasing CR, showing better thermal efficiency and fuel economy. The lowest SFC of 0.34794 kg/kWh is observed at a CR of 11.5. Torque and IMEP (Indicated Mean Effective Pressure): Torque and IMEP improve consistently with higher CR, enhancing the engine's ability to perform mechanical work. The maximum torque of 199.17 Nm and IMEP of 9.5324 bar occur at CR 11.5. NOx Emissions: NOx emissions rise with CR due to elevated peak combustion temperatures. For instance, NOx emissions increased from 0.651 ppm at CR 8.0 to 233.18 ppm at CR 11.5. Maximum Pressure (p_{max}): The peak pressure (p_{max}) rises as CR increases, signifying better combustion efficiency. However, this can stress engine components. The maximum p_{max} of 52.845 bar is recorded at CR 11.5. Thermal Efficiency (η_{TC}): While thermal efficiency improves with CR, the incremental gains reduce at higher CRs, with minimal improvements beyond CR 10.5. Airflow and Volumetric Efficiency (m_{air} , η_{v}): Airflow and volumetric efficiency remain steady across different CRs, indicating consistent air intake regardless of CR. Piston Temperature ($T_{w_{pist}}$): Piston temperature increases with CR, reaching a peak of 452.15 K at CR 11.5. This may require enhanced cooling mechanisms.

EGR Percentage (A_{egr}): The EGR percentage slightly reduces with higher CR, reflecting lower exhaust recirculation needs as thermal efficiency improves. Optimal Choice: CR = 10.5. This CR offers a balanced performance with a power output of 30.77 kW, torque of 195.92 Nm, and SFC of 0.35388 kg/kWh, while keeping NOx emissions (250.86 ppm), peak pressure (47.197 bar), and piston temperature (448.06 K) manageable. CR = 10.5 provides a good compromise between engine performance, fuel efficiency, and durability. If higher performance is prioritized, CR = 11.0 or 11.5 may be considered, though advanced cooling and robust materials would be required to handle increased thermal and mechanical stresses. The significance of this research lies in its potential to contribute to the development of cleaner and more efficient internal combustion engines by optimizing key parameters for the use of renewable fuels. By focusing on an 80% hydrogen and 20% ethanol blend in a Spark Ignition Engine, the study provides valuable insights into how engine performance can be enhanced through the optimal selection of compression ratio, ignition timing, and exhaust gas recirculation (EGR) ratio. The findings suggest that this blend could offer a viable alternative to conventional fossil fuels, reducing emissions, improving thermal efficiency, and enhancing overall engine power output. Additionally, this research highlights the importance of balancing engine parameters to achieve optimal fuel economy and performance, addressing challenges in adopting alternative fuels in internal combustion engines. The work supports the broader goals of sustainable transportation and energy systems, offering a pathway toward reducing reliance on petroleum-based fuels and minimizing the environmental impact of automotive emissions.

4.2 This research is important for several key reasons

Sustainability and Emission Reduction: As global concerns over climate change and air pollution grow, finding sustainable alternatives to fossil fuels is critical. The use of hydrogen-ethanol blends in internal combustion engines can significantly reduce harmful emissions such as CO₂ and NOx, contributing to cleaner air and a healthier environment.

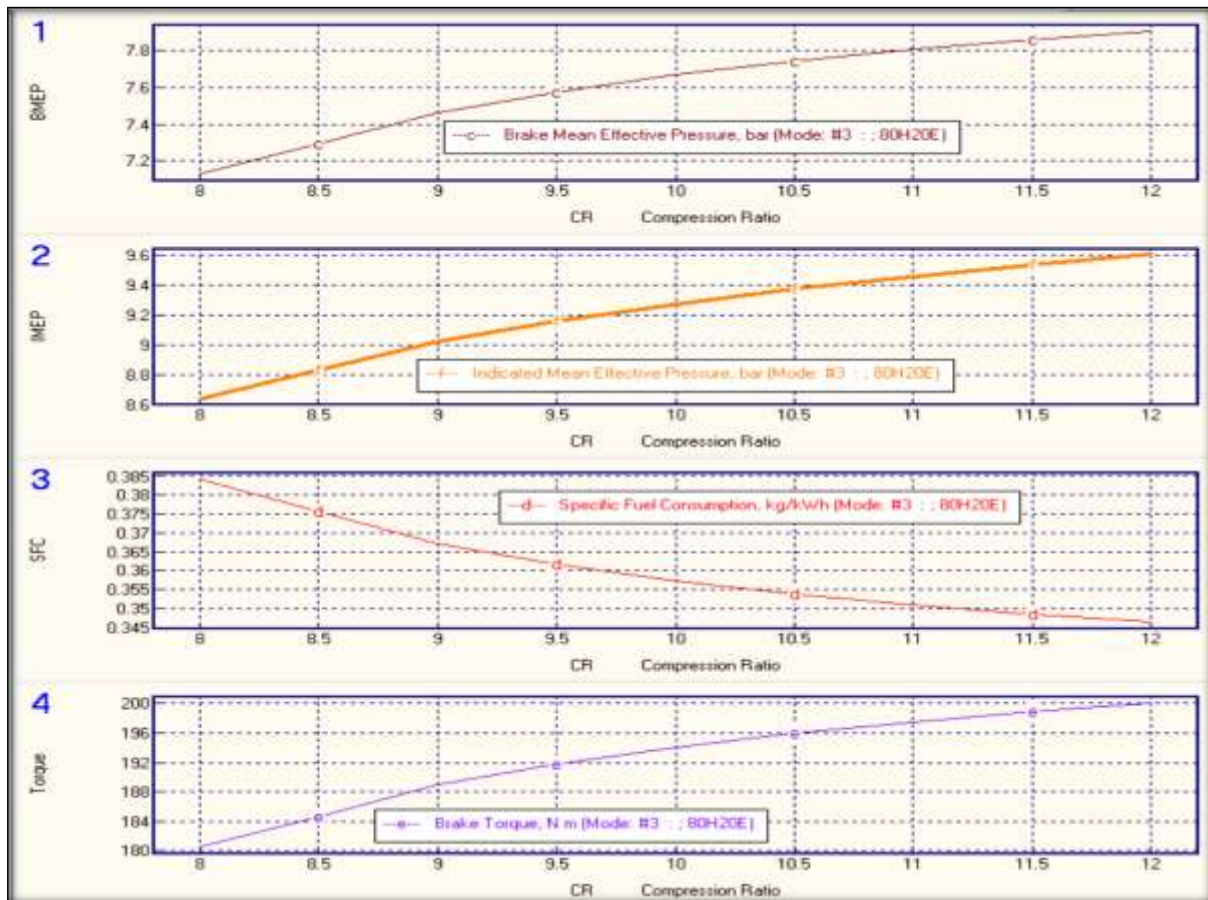


Figure 3 Performance Parameters like BMEP, IMEP, SFC, and P_eng comparison with variable CR.

Figure 3 shows that the Optimizing Engine Performance: By optimizing key engine parameters like compression ratio, ignition timing, and exhaust gas recirculation (EGR) ratio, the research offers insights into how engine efficiency and power output can be enhanced when using renewable fuels shown in Fig.3. This contributes to improved fuel economy and performance, making alternative fuels more viable in everyday automotive applications. Alternative Fuel Viability: The research investigates the performance of an 80% hydrogen and 20% ethanol blend, which holds promise as a viable alternative fuel combination. Understanding how to maximize its benefits through optimized engine settings could help accelerate its adoption in the transportation industry.

1. **Energy Security:** Hydrogen, as a fuel, offers a pathway toward reducing dependency on oil and other non-renewable resources. This research can provide the foundation for further developments in hydrogen infrastructure and its widespread integration into the automotive sector, enhancing energy security.
2. **Technological Innovation:** This study contributes to the ongoing innovation in engine design and fuel management, focusing on hybrid fuels and optimized engine systems. The findings could influence future research and development efforts, pushing the boundaries of what is possible in terms of engine performance, fuel efficiency, and environmental impact.

In summary, the importance of this research lies in its potential to advance the development of alternative fuels, improve engine performance, reduce emissions, and contribute to the global shift towards sustainable energy systems in the automotive sector.

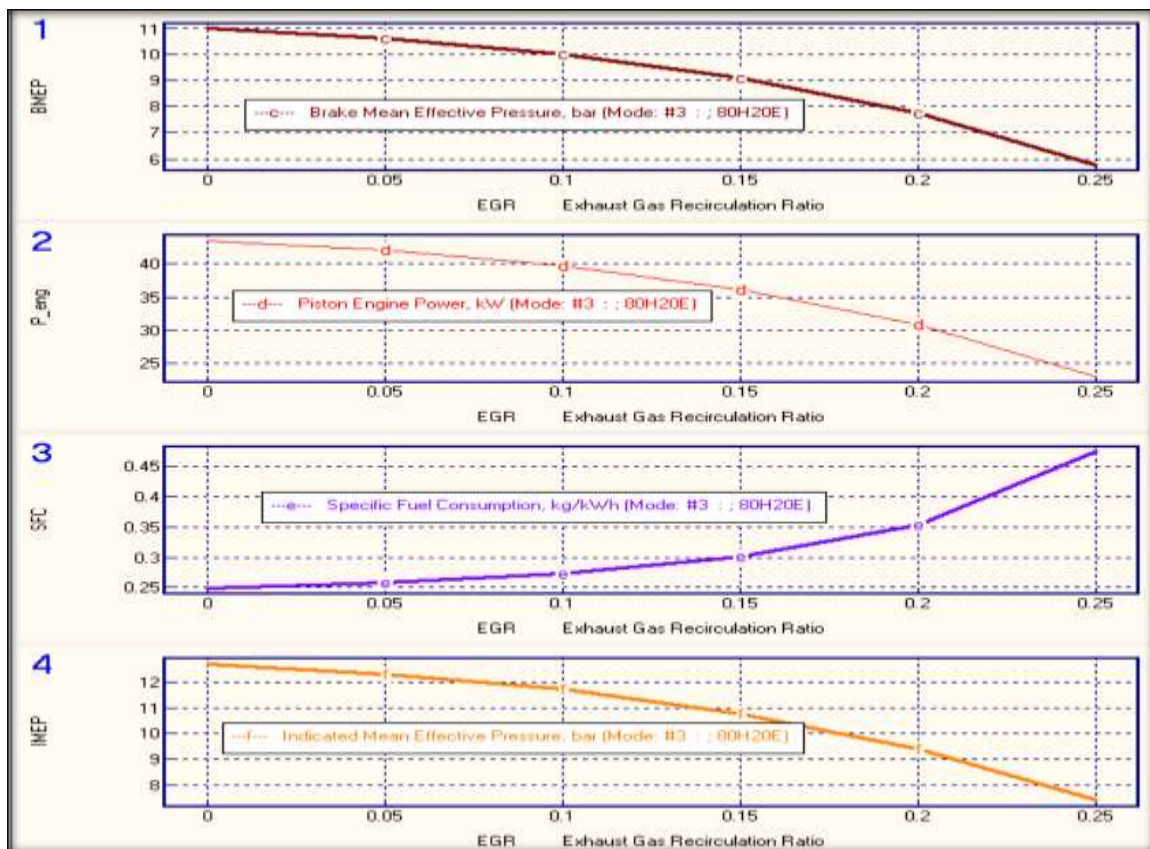


Figure 4 Performance Parameters like BMEP, IMEP, SFC, and P_{eng} comparison with variable EGR

Figure 4 shows the analysis of compression ratios (CR) highlighting their critical impact on engine performance, efficiency, and emissions. Increasing CR enhances engine power output, thermal efficiency, and torque, while reducing specific fuel consumption (SFC), demonstrating improved fuel economy. However, higher CRs also lead to elevated NO_x emissions, peak pressures, and piston temperatures, which pose challenges to engine durability and emissions control. The study concludes that a compression ratio of 10.5 is the optimal choice, offering a balanced trade-off between performance and efficiency. At CR = 10.5, the engine achieves significant power output and torque while maintaining manageable NO_x emissions and thermal stresses. Although CR = 11.5 provides the best performance metrics, it requires advanced materials and cooling strategies to mitigate the associated thermal and mechanical challenges. This evaluation underscores the importance of selecting a suitable compression ratio based on specific application requirements, ensuring an effective balance between performance, fuel efficiency, and long-term engine reliability. The graph shows a clear downward trend in NO_x emissions as the Exhaust Gas Recirculation (EGR) ratio increases. This is expected, as EGR is a well-established technique for reducing NO_x formation. Initial NO_x Level: At 0% EGR, the NO_x emissions are relatively high. This suggests that the combustion process under these conditions produces a significant amount of NO_x. NO_x Reduction with EGR: As the EGR ratio is increased, NO_x emissions decrease significantly. This indicates that the presence of recirculated exhaust gases in the combustion chamber disrupts the formation of NO_x. Possible Explanations for NO_x Reduction: Reduced Peak Temperatures: EGR dilutes the incoming air-fuel mixture with cooler exhaust gases, leading to a reduction in peak combustion temperatures. Since NO_x formation is highly temperature-dependent, lower temperatures inhibit its formation. Oxygen Dilution: EGR introduces inert gases (like CO₂ and N₂) into the combustion chamber, diluting the oxygen concentration. This

reduces the amount of oxygen available for the oxidation of nitrogen to form NO_x. Radical Scavenging: EGR gases contain species like CO and H₂, which can act as radical scavengers. These species can react with the free radicals involved in the NO_x formation process, thereby inhibiting its formation. Overall, the graph demonstrates the effectiveness of EGR in reducing NO_x emissions during the combustion of 80% hydrogen + 20% ethanol fuel. This is a crucial finding for the development of cleaner and more sustainable combustion systems.

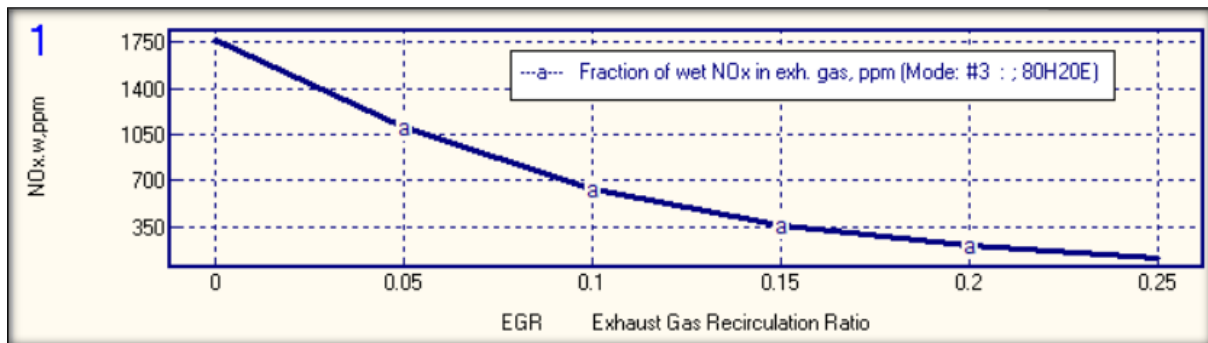


Figure 5 NO_x Comparison with variable EGR ratios

From Fig 5 shows the graph depicting the NO_x emissions during the combustion of 80% hydrogen + 20% ethanol fuel. Observations from the Graph: NO_x Trend: The graph shows a clear downward trend in NO_x emissions as the Exhaust Gas Recirculation (EGR) ratio increases. This is expected, as EGR is a well-established technique for reducing NO_x formation. Initial NO_x Level: At 0% EGR, the NO_x emissions are relatively high. This suggests that the combustion process under these conditions produces a significant amount of NO_x. NO_x Reduction with EGR: As the EGR ratio is increased, NO_x emissions decrease significantly. This indicates that the presence of recirculated exhaust gases in the combustion chamber disrupts the formation of NO_x. Possible Explanations for NO_x Reduction: Reduced Peak Temperatures: EGR dilutes the incoming air-fuel mixture with cooler exhaust gases, leading to a reduction in peak combustion temperatures. Since NO_x formation is highly temperature-dependent, lower temperatures inhibit its formation. Oxygen Dilution: EGR introduces inert gases (like CO₂ and N₂) into the combustion chamber, diluting the oxygen concentration. This reduces the amount of oxygen available for the oxidation of nitrogen to form NO_x. Radical Scavenging: EGR gases contain species like CO and H₂, which can act as radical scavengers. These species can react with the free radicals involved in the NO_x formation process, thereby inhibiting its formation. Overall, the graph demonstrates the effectiveness of EGR in reducing NO_x emissions during the combustion of 80% hydrogen + 20% ethanol fuel. This is a crucial finding for the development of cleaner and more sustainable combustion systems.

Additional Considerations:

- EGR Limits: While EGR is effective in reducing NO_x, excessive EGR can lead to other issues like incomplete combustion, increased soot formation, and reduced engine efficiency.
- Fuel Composition: The NO_x emissions characteristics can be influenced by the specific composition of the hydrogen-ethanol blend. Further investigation with different blend ratios might be warranted.
- Combustion Conditions: Other combustion parameters, such as equivalence ratio, residence time, and mixing intensity, can also affect NO_x emissions and the effectiveness of EGR.

5.0 UNCERTAINTY ANALYSIS

The engine parameters presented include various values along with their respective relative and absolute uncertainties, reflecting the precision of each measurement. The Compression Ratio (CR) is 8, with an absolute uncertainty of 0.08. The Equivalence Air-Fuel Ratio (A/F_{eq}) is 0.62751, accompanied by an

absolute uncertainty of 0.0062751. The Engine Power (P_{eng}) is measured at 28.343 kW, with an uncertainty of 0.28343 kW. The Specific Fuel Consumption (SFC) is 0.38422 kg/kWh, with a corresponding uncertainty of 0.0038422 kg/kWh. Torque is 180.45 Nm, with an uncertainty of 1.8045 Nm, and the Indicated Mean Effective Pressure (IMEP) is 8.6463 bar, carrying an uncertainty of 0.086463 bar.

Table 4: Uncertainty Analysis Data

Parameter	Value	Relative Uncertainty	Absolute Uncertainty
CR	8	0.01	0.08
A/F eq	0.62751	0.01	0.0062751
P_{eng} (kW)	28.343	0.01	0.28343
SFC (kg/kWh)	0.38422	0.01	0.0038422
Torque (Nm)	180.45	0.01	1.8045
IMEP (bar)	8.6463	0.01	0.086463
ON	76.416	0.01	0.76416
p_{max} (bar)	34.099	0.01	0.34099
Φ_z ($^\circ$)	59	0.01	0.59
dp/dTheta	0.71318	0.01	0.0071318
m_{air} (kg/s)	0.036327	0.01	0.00036327

From Table 4 shows that the Octane Number (ON) is 76.416, with an uncertainty of 0.76416, and the Maximum Pressure (p_{max}) is 34.099 bar, with an uncertainty of 0.34099 bar. The Crank Angle (Φ_z) is recorded at 59° , with a corresponding uncertainty of 0.59° . The Pressure Gradient (dp/dTheta) is 0.71318 bar/ $^\circ$, carrying an uncertainty of 0.0071318 bar/ $^\circ$. Lastly, the Air Mass Flow Rate (m_{air}) is 0.036327 kg/s, with an uncertainty of 0.00036327 kg/s. These values provide a comprehensive overview of key engine parameters, reflecting both the measured values and the associated uncertainty for each.

CONCLUSION:

1. Decrease in Brake Mean Effective Pressure (BMEP):

The BMEP decreases as the EGR ratio increases. At an EGR ratio of 0%, the BMEP is approximately 10.8 bar, which drops to around 8.5 bar at an EGR ratio of 25%. This indicates a reduction in the engine's ability to produce effective pressure as more exhaust gases are recirculated. Decrease in Engine Power (P_{eng}): Engine power decreases significantly with increasing EGR ratio. At an EGR ratio of 0, the engine power is around 35.3 kW, while at an EGR ratio of 0.25, it drops to approximately 30.2 kW. This trend highlights the adverse effect of higher EGR on power output, reducing the engine's efficiency in converting fuel into power. Increase in Specific Fuel Consumption (SFC): Specific fuel consumption increases as the EGR ratio rises. At an EGR ratio of 0, SFC is about 0.27 kg/kWh, whereas at an EGR ratio of 0.25, it increases to approximately 0.44 kg/kWh. This suggests that higher EGR ratios lead to less efficient combustion, requiring more fuel to produce the same amount of power. Decrease in Indicated Mean Effective Pressure (IMEP): The IMEP also decreases with increasing EGR ratio. At an EGR ratio of 0, IMEP is around 12.1 bar, but at an EGR ratio of 0.25, it falls to roughly 9.4 bar. This drop in IMEP further supports the observation that higher EGR reduces the combustion efficiency inside the engine.

2. Trade-off between Performance and Emissions:

While increasing the EGR ratio helps in reducing nitrogen oxide (NO_x) emissions, it comes at the expense of engine performance. For example, a higher EGR ratio of 0.25 leads to a significant reduction in power and pressure but could lower NO_x emissions, making it a trade-off between performance and emission control.

3. Optimal EGR Ratio for Balance:

Based on the data, an optimal EGR ratio appears to be around 0.1 to 0.15, where engine power and fuel consumption are reasonably balanced. For instance, at an EGR ratio of 0.1, the engine power is about 33.5 kW, and SFC is approximately 0.33 kg/kWh. This range offers a compromise between maintaining reasonable engine performance and reducing emissions.

Acknowledgment

The authors would like to express their sincere gratitude to Dr. A. Karthikeyan, Dr. M. Karthikeyan, and Dr. G. Sureshkannan, Assistant Professors and Associate Professors, Department of Mechanical Engineering, Coimbatore Institute of Technology, Coimbatore-14, for their invaluable guidance, support, and encouragement throughout the course of this work. The authors also extend their heartfelt thanks to the Principal of Coimbatore Institute of Technology and Management for providing the necessary facilities, resources, and support to carry out this research successfully.

NOMENCLATURE

- Compression Ratio
- **BMEP**: Brake Mean Effective Pressure (bar)
- **P_{eng}**: Piston Engine Power (kW)
- **Torque**: Brake Torque (N·m)
- **SFC**: Specific Fuel Consumption (kg/kWh)
- **IMEP**: Indicated Mean Effective Pressure (bar)
- **A/F_{eq}**: Air-Fuel Equivalence Ratio (Lambda) in the Cylinder
- **To_T**: Average Total Turbine Inlet Temperature (K)
- **Tw_{pist}**: Average Piston Crown Temperature (K)
- **P_{inj,max}**: Maximum Sac Injection Pressure (before nozzles) (bar)
- **d₃₂**: Sauter Mean Diameter of Drops (microns)
- **Phi_{ign}**: Ignition Delay Period (degrees)
- **P_{max}**: Maximum Cylinder Pressure (bar)
- **dp/dTheta**: Maximum Rate of Pressure Rise (bar/degree)
- **Phi_z**: Combustion Duration (degrees)
- **m_{air}**: Total Mass Airflow (+EGR) of Piston Engine (kg/s)
- **Eta_v**: Volumetric Efficiency
- **x_r**: Residual Gas Mass Fraction
- **PMEP**: Pumping Mean Effective Pressure (bar)
- **Eta_{TC}**: Turbocharger Efficiency
- **BF_{int}**: Burnt Gas Fraction Back flowed into the Intake (%)
- **NO_x .ppm**: Fraction of Wet NO_x in Exhaust Gas (ppm)
- **PM**: Specific Particulate Matter Emission (g/kWh)
- **Bosch**: Bosch Smoke Number
- **SE**: Summary of Emissions of PM and NO_x
- **A_{egr}**: Effective Area of EGR Discharge Holes (mm²)
- **dp_{ev}**: Differential Pressure between Exhaust Manifold and Venturi Throat (bar)
- **P_{C.hp}**: Power of High-Pressure Compressor (HPC) (kW)
- **To_{C.hp}**: Total Temperature After Intercooler (K)

- **PR_T.hp**: Expansion Pressure Ratio of High-Pressure Turbine (HPT)
- **Eta_T.hp**: Internal Turbine Efficiency of High-Pressure Turbine
- **P_T.hp**: Effective Power of High-Pressure Turbine (kW)
- **p_o.I.hp**: Inlet Total Pressure of High-Pressure Turbine (bar)
- **To_I.hp**: Inlet Total Temperature of High-Pressure Turbine (K)
- **RPM_C.hp**: HP Stage Turbocharger Rotor Speed (rpm)

References

1. Al-Hasan, M., & Al-Momany, M. (2008). The effect of ethanol-unleaded gasoline blends on engine performance and exhaust emissions. *Renewable Energy*, 33(1), 27–33.
2. Geng, P., Cao, E., Tan, Q., & Wei, L. (2017). Effects of alternative fuels on the combustion characteristics and emissions of internal combustion engines: A review. *Renewable and Sustainable Energy Reviews*, 71, 523–534.
3. Bari, S., & Esmail, M. M. (2010). Engine performance and emission reduction using dual fuel with hydrogen and gasoline. *International Journal of Hydrogen Energy*, 35(21), 12005–12014.
4. Li, H., Lu, J., & Wang, J. (2017). Performance and emissions of a spark-ignition engine using ethanol-hydrogen blended fuels. *International Journal of Hydrogen Energy*, 42(10), 6628–6637.
5. Abdel-Rahman, A. A., & Osman, M. M. (1997). Experimental investigation on varying the compression ratio of SI engine working under different ethanol-gasoline fuel blends. *International Journal of Energy Research*, 21(1), 31–40.
6. Hsieh, W. D., Chen, R. H., Wu, T. L., & Lin, T. H. (2002). Engine performance and pollutant emission of an SI engine using ethanol-gasoline blended fuels. *Atmospheric Environment*, 36(3), 403–410.
7. Verhelst, S., & Wallner, T. (2009). Hydrogen-fueled internal combustion engines. *Progress in Energy and Combustion Science*, 35(6), 490–527.
8. Wu, H. W., Lin, B. F., Chen, Y. C., & Lee, T. H. (2011). Optimized engine performance and hydrocarbon emissions of an SI engine using ethanol-gasoline blended fuels. *Atmospheric Environment*, 45(26), 4194–4200.
9. Qi, D., Chen, H., & Xu, H. (2013). Combustion and emission characteristics of ethanol-blended diesel fuel. *Renewable Energy*, 51, 60–65.
10. Mahla, S. K., & Chauhan, B. S. (2018). Effects of EGR and ignition timing on performance of an SI engine fueled with hydrogen-blended ethanol. *International Journal of Hydrogen Energy*, 43(28), 12791–12800.
11. Jothi, N. K., Nagarajan, G., & Renganarayanan, S. (2007). LPG fueled diesel engine using diethyl ether with exhaust gas recirculation. *International Journal of Hydrogen Energy*, 32(15), 4501–4509.
12. Najafi, G., Ghobadian, B., & Tavakoli, T. (2009). Performance and exhaust emissions of a gasoline engine with ethanol blends. *Applied Thermal Engineering*, 29(8-9), 1818–1824.
13. Pal, P., & Sen, S. (2018). Impact of hydrogen and ethanol blending on the performance of an SI engine. *International Journal of Hydrogen Energy*, 43(12), 6338–6348.
14. Milton, B. E., & Keck, J. C. (1984). Laminar burning velocities in stoichiometric hydrogen and hydrogen-hydrocarbon gas mixtures. *Combustion and Flame*, 58(1), 13–22.
15. Kim, S. M., & Lee, S. (2013). Optimization of ignition timing for hydrogen-blended ethanol engines. *International Journal of Hydrogen Energy*, 38(13), 5614–5624.
16. Rakopoulos, C. D., & Dimaratos, A. M. (2009). Combustion and emission characteristics of dual fuel compression ignition engine using natural gas. *Energy Conversion and Management*, 50(11), 2924–2933.
17. Matthews, R. D., & Blaxill, H. (2008). The influence of ethanol on spark-ignition engine combustion performance. *SAE Technical Paper 2008-01-1777*.
18. Zhao, F., Lai, M. C., & Harrington, D. L. (1999). Automotive spark-ignited direct-injection gasoline engines. *Progress in Energy and Combustion Science*, 25(5), 437–562.

19. Çelik, M. B. (2008). Experimental determination of suitable ethanol-gasoline blend rate at high compression ratio for gasoline engine. *Applied Thermal Engineering*, 28(4), 396–404.
20. Akansu, S. O., Dulger, Z., Kahraman, N., & Veziroglu, T. N. (2007). Internal combustion engines fueled by natural gas-hydrogen mixtures. *International Journal of Hydrogen Energy*, 32(4), 427–435.
21. Gautam, M., Martin, D. W., & Carder, D. K. (2000). Emissions characteristics of higher alcohol/gasoline blends. *Proceedings of the Institution of Mechanical Engineers, Part D: Journal of Automobile Engineering*, 214(2), 165–182.
22. Goldsworthy, L., & McMillan, P. (2008). Effects of hydrogen addition on the combustion of methane and natural gas in spark ignition engines. *Fuel*, 87(7), 1013–1021.
23. Stone, R. (2012). *Introduction to Internal Combustion Engines* (4th ed.). Palgrave Macmillan.
24. Bakar, R. A., Ali, M. H., & Rajoo, S. (2008). Combustion characteristics of a hydrogen-fueled SI engine. *International Journal of Hydrogen Energy*, 33(8), 3320–3328.
25. Shudo, T., & Kihara, R. (2001). Suppression of knocking by hydrogen-rich reformat gas in SI engines. *International Journal of Hydrogen Energy*, 26(7), 661–665.
26. Arsie, I., Pianese, C., & Sorrentino, M. (2009). A quasi-dimensional combustion model for engine control applications. *Energy Conversion and Management*, 50(1), 93–102.
27. Homan, H., Al-Riyami, M., & Chandrasekhar, A. (2011). Effects of exhaust gas recirculation on NOx reduction in hydrogen and ethanol blend engines. *SAE Technical Paper 2011-01-2348*.
28. Rahman, S. M. A., & Masjuki, H. H. (2009). Combustion analysis of alcohol-gasoline blends in SI engines. *Energy*, 34(12), 1974–1981.
29. Szybist, J. P., & Splitter, D. A. (2010). Comparison of hydrogen addition to gasoline, ethanol, and methane fuels. *International Journal of Hydrogen Energy*, 35(19), 11095–11105.
30. Heywood, J. B. (2018). *Internal Combustion Engine Fundamentals* (2nd ed.). McGraw-Hill Education.